

Noise-Induced Spatial Pattern Formation in Stochastic Reaction-Diffusion Systems *

Yutaka Hori

Shinji Hara [†]

Abstract

This paper is concerned with stochastic reaction-diffusion kinetics governed by the reaction-diffusion master equation. Specifically, the primary goal of this paper is to provide a mechanistic basis of Turing pattern formation that is induced by intrinsic noise. To this end, we first derive an approximate reaction-diffusion system by using linear noise approximation. We show that the approximated system has a certain structure that is associated with a coupled dynamic multi-agent system. This observation then helps us derive an efficient computation tool to examine the spatial power spectrum of the intrinsic noise. We numerically demonstrate that the result is quite effective to analyze noise-induced Turing pattern. Finally, we illustrate the theoretical mechanism behind the noise-induced pattern formation with a \mathcal{H}_2 norm interpretation of the multi-agent system.

1 Introduction

The auto-regulation mechanism of the biological pattern formation is a long standing question in biology. It was Turing [1] who first presented a mathematical model that possibly accounts for the pattern formation in embryonic development. Specifically, it was shown that a pair of reaction-diffusion equations can spontaneously exhibit spatial structure after a small perturbation to a spatially homogeneous equilibrium. Nowadays, such patterns are called Turing pattern, and analysis ranges to a wide variety of biological applications (see [2] for example).

Although many existing studies rely on deterministic reaction-diffusion models, intrinsic noise is often a unignorable factor leading to a drastic change of the dynamics [3]. It is known that the dynamics of stochastic chemical reactions in a cell follows the chemical master equation (CME) [4]. A standing assumption of the CME is that reactants are well-mixed in a cell. However, recent studies revealed that molecules can localize inside a cell, and the localization plays an important role, for example, in cell division [5]. Hence, it is important to analyze the stochastic dynamics of biochemical reactions under the spatially inhomogeneous environment.

*©2012 IEEE. Personal use of this material is permitted. Permission from IEEE must be obtained for all other uses, in any current or future media, including reprinting/republishing this material for advertising or promotional purposes, creating new collective works, for resale or redistribution to servers or lists, or reuse of any copyrighted component of this work in other works. The citation of this work should be as follows: Y. Hori and S. Hara, “Noise-Induced Spatial Pattern Formation in Stochastic Reaction-Diffusion Systems,” *Proceedings of IEEE Conference on Decision and Control*, pp. 1053–1058, 2012.

[†]Y. Hori and S. Hara are with Department of Information Physics and Computing, The University of Tokyo, 7-3-1 Hongo, Bunkyo-ku, Tokyo 113-8656, Japan. {Yutaka.Hori, Shinji.Hara}@ipc.i.u-tokyo.ac.jp

The reaction-diffusion master equation (RDME) [6] describes the dynamics of the molecular copy numbers under the stochastic reaction-diffusion process. In this formulation, the spatial domain is partitioned into small voxels so that the molecules are well-mixed inside each voxel, but the copy numbers of molecules are small enough to preserve the stochasticity. Thus, the dynamics of reactions inside each voxel is governed by the chemical master equation (CME) [4], while the diffusion is modeled as the exchange of the molecules between voxels.

In [7], the stochastic pattern formation was studied for Brusselator [8] based on the RDME. Interestingly, it was observed that Brusselator can exhibit spatial patterns even when the deterministic reaction-diffusion model converges to a homogeneous equilibrium. This implies that intrinsic fluctuation drives a particular spatial mode, and results in inhomogeneous spatial structure. This research thereafter inspired the investigation of the noise-induced Turing patterns in Levin-Segel model [9] and the noise-induced spatio-temporal oscillations in Brusselator [10].

In these papers [7, 9, 10], an approximate model obtained by linear noise approximation (LNA) [11] was used to compute the spatial power spectrum of the patterns. Later, the LNA for reaction-diffusion systems was formulated in a more general form in [12], and the analytic results obtained by the approximation agreed with the stochastic simulations. Although these methods were shown to give a good approximation, the mechanistic basis of the stochastic pattern formation is not necessarily revealed. Hence, it is desirable that the system be analyzed from a system theoretic viewpoint to understand the mechanism behind the phenomenon.

The goal of this paper is to provide a mechanistic understanding of the stochastic reaction-diffusion system, and to reveal the mechanism of the noise-induced Turing pattern from a control theoretic viewpoint. Specifically, it is shown that the computation of the covariance of intrinsic noise can be viewed as the \mathcal{H}_2 norm computation of a coupled dynamic multi-agent system, where disturbance inputs are injected to each agent's states and sensed outputs. Then, an efficient method to compute the spatial power spectrum is derived by using the characteristic structure of the reaction-diffusion system. Using these analytic tools, we analyze noise-induced Turing patterns observed in the celebrated Gray-Scott model [13, 14]. It should be remarked that to the authors' knowledge, this paper gives the first presentation of the noise-induced Turing pattern in the Gray-Scott model [13, 14]. Finally, we reveal the mechanism of the noise-induced pattern formation with the \mathcal{H}_2 norm interpretation of the multi-agent system.

This paper is organized as follows. In the next section, the RDME is briefly presented. Then, an approximated system of the RDME is derived by using the LNA in Section III. In Section IV, the characteristic structure of the approximated system is revealed, and its control theoretic interpretation is presented. Furthermore, an efficient method to compute spatial power spectrum is obtained. In Section V, noise-induced Turing patterns are demonstrated with the Gray-Scott model, and their mechanism is illustrated. Finally, the paper is concluded in Section VI.

2 Model description of stochastic reaction-diffusion systems

In this section, the dynamics of stochastic reaction-diffusion system, which we call reaction-diffusion master equation (RDME) [6] is introduced.

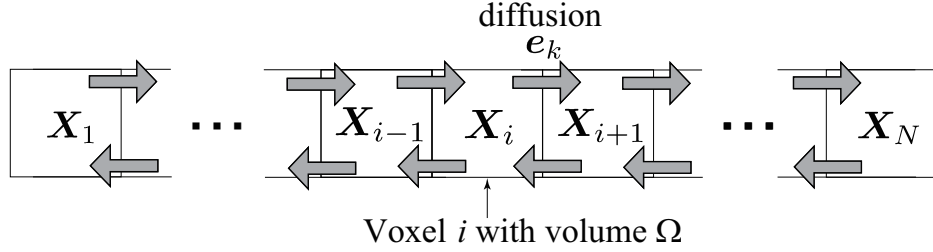


Figure 1: The reaction-diffusion scheme considered in the RDME formulation.

Consider a set of chemical reactions that consists of n molecular species, $\mathcal{M}_1, \mathcal{M}_2, \dots, \mathcal{M}_n$, and m_0 reactions, $\mathcal{R}_1, \mathcal{R}_2, \dots, \mathcal{R}_{m_0}$, in a spatial domain. Suppose the domain is partitioned into N voxels, $\mathcal{V}_1, \mathcal{V}_2, \dots, \mathcal{V}_N$ with the same volume Ω . It is assumed that molecules are well-mixed within each voxel, and can react with those in the same voxel. Figure 1 shows an example of the situation for one dimensional case.

Let an integer vector $\mathbf{X}_i \in \mathbb{Z}_+^n$ denote the copy number of molecular species inside the voxel \mathcal{V}_i ($i = 1, 2, \dots, N$). Stacking the vector \mathbf{X}_i , we define

$$\mathbf{X} := [\mathbf{X}_1^T, \mathbf{X}_2^T, \dots, \mathbf{X}_N^T]^T \in \mathbb{Z}_+^{nN}. \quad (1)$$

It is known that the stochastic time development of the molecular copy number follows the chemical master equation (CME) for well-mixed chemical systems [4]. Thus, the dynamics of chemical reactions inside the voxel \mathcal{V}_i is given by

$$\begin{aligned} \frac{\partial P(\mathbf{X}_i, t)}{\partial t} &= \sum_{r=1}^{m_0} (w_r(\mathbf{X}_i - \mathbf{s}_r) P(\mathbf{X}_i - \mathbf{s}_r, t) \\ &\quad - w_r(\mathbf{X}_i) P(\mathbf{X}_i, t)) = \mathcal{A}_i P(\mathbf{X}_i, t), \end{aligned} \quad (2)$$

where $P(\mathbf{X}_i, t)$ denotes the conditional probability that there are \mathbf{X}_i molecules in \mathcal{V}_i at time t for a given initial state and time ¹. The function $w_r(\cdot) : \mathbb{Z}_+^n \rightarrow \mathbb{R}_+$ ($r = 1, 2, \dots, m_0$) and the vector $\mathbf{s}_r \in \mathbb{Z}^n$ denote the propensity function and stoichiometry for the reaction \mathcal{R}_r (see [15] for details). We define \mathcal{A}_i as an infinitesimal generator describing the development of $P(\mathbf{X}_i, t)$.

The diffusion of molecules can be modeled by the exchange of molecules between voxels (see Fig. 1). When one molecule of \mathcal{M}_k moves from the voxel \mathcal{V}_i to \mathcal{V}_j , the number of molecules \mathbf{X} changes to $[\mathbf{X}_1^T, \dots, \mathbf{X}_i^T - \mathbf{e}_k^T, \dots, \mathbf{X}_j^T + \mathbf{e}_k^T, \dots, \mathbf{X}_N^T]^T$, where $\mathbf{e}_k := [0, \dots, 0, 1, 0, \dots, 0] \in \mathbb{Z}^n$ is the standard unit vector with 1 at the k -th entry. Let \mathcal{I}_i ($i = 1, 2, \dots, N$) denote a set of adjacent voxels of \mathcal{V}_i , *i.e.*,

$$\mathcal{I}_i := \{j \in \{1, 2, \dots, N\} \mid \mathcal{V}_j \text{ is adjacent to } \mathcal{V}_i\}. \quad (3)$$

In general, \mathbf{X} is updated as

$$\mathbf{X} + \mathbf{v}_{ij} \otimes \mathbf{e}_k, \quad (4)$$

¹More precisely, $P(\mathbf{X}_i, t)$ should be written as $P(\mathbf{X}_i, t | \mathbf{X}_{i_0}, t_0)$ with the initial state \mathbf{X}_{i_0} and time t_0 . In this paper, however, we omit the condition, and simply write $P(\mathbf{X}_i, t)$ to avoid notational complexity.

for each diffusion event, where the vector $\mathbf{v}_{ij} \in \mathbb{Z}^N$ has -1 at the i -th entry, $+1$ at the j -th entries ($j \in \mathcal{I}_i$) and 0 at the other entries. Thus, the dynamics of diffusion is written as

$$\begin{aligned} \frac{\partial P(\mathbf{X}, t)}{\partial t} &= \sum_{i=1}^N \sum_{j \in \mathcal{I}_i} \sum_{k=1}^n (\delta_k(X_i + 1) P(\mathbf{X} - \mathbf{v}_{ij} \otimes \mathbf{e}_k, t) \\ &\quad - \delta_k X_i P(\mathbf{X}, t)) = \mathcal{D}P(\mathbf{X}, t), \end{aligned} \quad (5)$$

where $P(\mathbf{X}, t)$ is the conditional probability that there are \mathbf{X} molecules at time t for a given initial state and time. The diffusion constant of the molecule \mathcal{M}_k is defined by $\delta_k := d_k/\ell^2$ with a deterministic diffusion rate $d_k > 0$ and the characteristic length of each voxel ℓ . The probability that one molecule of \mathcal{M}_k moves from \mathcal{V}_i to an adjacent voxel within a small time interval $[t, t + \Delta t]$ is given by $\delta_k X_i \Delta t$. We define \mathcal{D} as the infinitesimal generator that accounts for diffusion.

From (2) and (5), we have the following reaction-diffusion master equation (RDME).

$$\frac{\partial P(\mathbf{X}, t)}{\partial t} = \sum_{i=1}^N \mathcal{A}_i P(\mathbf{X}_i, t) + \mathcal{D}P(\mathbf{X}, t). \quad (6)$$

Although the RDME describes the dynamics of intrinsic noise in stochastic reaction-diffusion systems, it is known that the RDME is hard to solve analytically in most cases. Hence, in the next section, we introduce an approximation method to understand the properties of the intrinsic noise in an analytic way. We hereafter restrict our attention to one dimensional spatial domain for simplicity. The theoretical results, however, can be extended to higher dimensional cases in a similar approach.

3 Linear noise approximation

In this section, we briefly describe the idea of linear noise approximation [11], and derive the approximated dynamics of (6).

Let $\mathbf{x}^\Omega := \mathbf{X}/\Omega \in \mathbb{R}_+^{nN}$ denote the concentration of molecules. Note that the molecular copy number \mathbf{X} divided by the volume Ω is the concentration. It is known that \mathbf{x}^Ω converges to a deterministic solution in the thermodynamic limit $\Omega \rightarrow \infty$ [16, 17]. Specifically, let

$$\mathbf{x}_i := \lim_{\Omega \rightarrow \infty} \frac{X_i}{\Omega} \quad (i = 1, 2, \dots, N), \quad (7)$$

and $\mathbf{x} := [\mathbf{x}_1^T, \mathbf{x}_2^T, \dots, \mathbf{x}_N^T]^T \in \mathbb{R}_+^{nN}$. Then, $\mathbf{x}(t)$ follows the spatially discretized reaction-diffusion equation

$$\dot{\mathbf{x}} = \begin{bmatrix} f(\mathbf{x}_1) \\ \vdots \\ f(\mathbf{x}_N) \end{bmatrix} + (L \otimes D)\mathbf{x} \quad (8)$$

with the initial value $\mathbf{x}(0) := \lim_{\Omega \rightarrow \infty} \mathbf{x}^\Omega(0)$, where L is defined by a discretized Laplacian matrix

$$L := \begin{bmatrix} -1 & 1 & 0 & \dots & 0 \\ 1 & -2 & 1 & \dots & \vdots \\ \vdots & \ddots & \ddots & \ddots & \vdots \\ 0 & \dots & 1 & -2 & 1 \\ 0 & \dots & 0 & 1 & -1 \end{bmatrix} \in \mathbb{R}^{N \times N} \quad (9)$$

and D is the deterministic diffusion rate matrix defined by

$$D := \text{diag}[d_1, d_2, \dots, d_n] \in \mathbb{R}^{n \times n} \quad (10)$$

with $d_i := \delta_i \ell^2$. In (9), the Neumann boundary condition with zero flux is assumed. Though the following argument can also be applied to the case where the boundary is periodic, we hereafter assume the Neumann boundary for simplicity.

As we have seen in (7), the variance of molecular copy number \mathbf{X}_i becomes less significant as the volume Ω becomes larger, and eventually converges to zero. Thus, one would expect from this observation that \mathbf{X}_i is approximated around the deterministic solution \mathbf{x}_i as

$$\mathbf{X}_i \simeq \Omega \mathbf{x}_i + \Omega^{\frac{1}{2}} \boldsymbol{\eta}_i \quad (i = 1, 2, \dots, N), \quad (11)$$

where $\boldsymbol{\eta}_i$ is a noise term whose properties are specified later. It should be noted that $\Omega \mathbf{x}_i$ is dimensionless, and the noise grows with $O(\Omega^{1/2})$.

Let $\boldsymbol{\eta} \in \mathbb{R}^{nN}$ be defined by

$$\boldsymbol{\eta} := [\boldsymbol{\eta}_1^T, \boldsymbol{\eta}_2^T, \dots, \boldsymbol{\eta}_N^T]^T \in \mathbb{R}^{nN}. \quad (12)$$

Note that the subscript of $\boldsymbol{\eta}$ stands for the index of a voxel. Since \mathbf{x}_i is a deterministic value obtained from (8), $\boldsymbol{\eta}$ is the only random variable that determines the stochastic fluctuations. Thus, defining $\Pi(\boldsymbol{\eta}, t)$ as the probability distribution of $\boldsymbol{\eta}$ at time t , we have $P(\mathbf{X}, t) \simeq \Omega^{-\frac{nN}{2}} \Pi(\boldsymbol{\eta}, t)$, where the scaling term comes from the change of variable of probability distribution. We see that the probability distribution $\Pi(\boldsymbol{\eta}, t)$ contains the property of intrinsic noise.

The idea of linear noise approximation [11] is that we replace \mathbf{X} in the equation (6) with the right-hand side of (11), and expand around the deterministic value $\Omega \mathbf{x}$ with Taylor expansion. Sorting with the power of Ω , we have the deterministic model (8) in the term of $\Omega^{1/2}$, and a Fokker-Planck equation of $\Pi(\boldsymbol{\eta}, t)$ in the term of Ω^0 . Since $O(\Omega^{-1/2})$ terms become less significant as Ω becomes large, we can approximately adopt the Fokker-Planck equation as the dynamics of $\Pi(\boldsymbol{\eta}, t)$. Then, the standard argument of stochastic systems allows us to see that $\boldsymbol{\eta}$ satisfies the following dynamic equation.

$$d\boldsymbol{\eta} = J_{\mathbf{x}(t)} \boldsymbol{\eta} dt + S W_{\mathbf{x}(t)}^{\frac{1}{2}} d\mathcal{B}(t), \quad (13)$$

where $\mathcal{B}(t)$ is a vector of $R := m_0 N + m_1 n$ independent standard Wiener process with $m_1 := \sum_{i=1}^N |\mathcal{I}_i|$. The matrix $J_{\mathbf{x}(t)} \in \mathbb{R}^{nN \times nN}$ is Jacobian of (8) at $\mathbf{x}(t)$. S and $W_{\mathbf{x}(t)}$ are defined as stoichiometry matrix and a diagonal matrix with the propensity functions at diagonal entries, which are specified from (6), respectively [15].

In the following section, we consider the stochastic fluctuation around a spatially homogeneous equilibrium point, at which stochastic Turing pattern is expected. In particular, a characteristic structure of the stochastic system (13) is revealed based on properties of the reaction-diffusion system.

4 Analysis of noise-induced spatial patterns

4.1 Structure of the stochastic system and noise covariance

Let $\mathbf{x}_e \in \mathbb{R}^n$ denote an equilibrium of $\dot{\mathbf{x}}_i = f(\mathbf{x}_i)$, where $f(\cdot)$ is given in the deterministic model defined in (8). We can see that $\mathbf{x}^* := [\mathbf{x}_e^T, \mathbf{x}_e^T, \dots, \mathbf{x}_e^T]^T \in \mathbb{R}_+^{nN}$ is a spatially homogeneous equilibrium point, *i.e.*, the values are the same between voxels.

Table 1: Meaning of the matrices

S_0	Stoichiometry matrix for $\mathcal{R}_1, \mathcal{R}_2, \dots, \mathcal{R}_{m_0}$
S_1	Incidence matrix of voxels
W_0	Diagonal matrix whose entries are propensity functions for $\mathcal{R}_1, \mathcal{R}_2, \dots, \mathcal{R}_{m_0}$.
W_1	Diagonal matrix whose entries are the equilibrium concentrations of $\mathcal{N}_1, \mathcal{N}_2, \dots, \mathcal{N}_n$.
D	Diagonal matrix whose entries are the diffusion rate of $\mathcal{N}_1, \mathcal{N}_2, \dots, \mathcal{N}_n$.

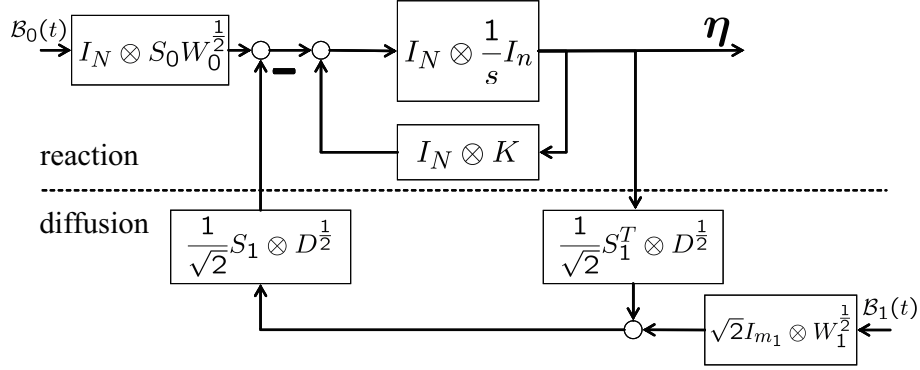


Figure 2: Block diagram of the stochastic system (13).

Using the structure of (6), it can be shown that the matrices in (13) are given by

$$\begin{aligned}
 J_{\mathbf{x}^*} &:= I_N \otimes K + L \otimes D \in \mathbb{R}^{nN \times nN}, \\
 S &:= [I_N \otimes S_0, S_1 \otimes I_n] \in \mathbb{Z}^{nN \times R}, \\
 W_{\mathbf{x}^*} &:= \begin{bmatrix} I_N \otimes W_0 & O \\ O & I_{m_1} \otimes DW_1 \end{bmatrix} \in \mathbb{R}_+^{R \times R},
 \end{aligned}$$

where

$$\begin{aligned}
 K &:= \left(\frac{\partial f}{\partial \mathbf{x}} \right) \bigg|_{\mathbf{x}=\mathbf{x}^*} \in \mathbb{R}^{n \times n} \\
 S_0 &:= [\mathbf{s}_1, \mathbf{s}_2, \dots, \mathbf{s}_{m_0}] \in \mathbb{Z}^{n \times m_0} \\
 S_1 &:= [\mathbf{v}_1, \mathbf{v}_2, \dots, \mathbf{v}_N] \in \mathbb{Z}^{N \times m_1} \\
 W_0 &:= \text{diag}(\hat{w}_1(\mathbf{x}_e), \hat{w}_2(\mathbf{x}_e), \dots, \hat{w}_{m_0}(\mathbf{x}_e)) \in \mathbb{R}^{m_0 \times m_0} \\
 W_1 &:= \text{diag}(x_e^{(1)}, x_e^{(2)}, \dots, x_e^{(n)}) \in \mathbb{R}^{n \times n}.
 \end{aligned}$$

The vector \mathbf{v}_i is $\mathbf{v}_i := [\mathbf{v}_{ij_1}, \mathbf{v}_{ij_2}, \dots, \mathbf{v}_{ij_{|\mathcal{I}_i|}}] \in \mathbb{Z}^{N \times |\mathcal{I}_i|}$ with $j_k \in \mathcal{I}_i$. The function $\hat{w}_i(\cdot) : \mathbb{R}_+^n \rightarrow \mathbb{R}_+$ is defined as the deterministic reaction rate for reaction \mathcal{R}_i , and $x_e^{(i)}$ is the i -th entry of \mathbf{x}_e ($i = 1, 2, \dots, n$). The meanings of each matrix are summarized in Table 1.

Substituting the above definition into (13), we see that the overall system has the structure shown in Fig. 2. Since the matrices S_0, W_0 and K are associated with the reactions inside each voxel, \mathcal{B}_0 excites the intrinsic noise arising from intravoxel reactions. On the other hand, \mathcal{B}_1 excites the one arising from diffusion (see Fig. 2).

It follows from (13) that the covariance of the noise $\mathbb{E}[\boldsymbol{\eta}\boldsymbol{\eta}^T]$ at the steady state \mathbf{x}^* is given by the Lyapunov equation

$$J_{\mathbf{x}^*}\Sigma + \Sigma J_{\mathbf{x}^*}^T + S W_{\mathbf{x}^*} S^T = 0. \quad (14)$$

Thus, we have the following proposition.

Proposition 1. *Consider the system (13). Suppose the spatially homogeneous equilibrium \mathbf{x}^* is locally stable. The steady state covariance of the noise $\Sigma := \mathbb{E}[\boldsymbol{\eta}\boldsymbol{\eta}^T]$ is given by the positive definite solution of the Lyapunov equation*

$$\begin{aligned} (I_N \otimes K + L \otimes D)\Sigma + \Sigma(I_N \otimes K^T + L \otimes D) \\ + (I_N \otimes S_0 W_0 S_0^T - 2L \otimes D W_1) = 0 \end{aligned} \quad (15)$$

This proposition provides an approximation of the covariance of the intrinsic noise whose dynamics is given by (13). The i -th n by n diagonal block of Σ stands for the covariance inside the voxel \mathcal{V}_i , i.e., $\mathbb{E}[\boldsymbol{\eta}_i \boldsymbol{\eta}_i^T]$. The covariance between voxels appears in off-diagonal entries, where the (i, j) off-diagonal block is defined by $\mathbb{E}[\boldsymbol{\eta}_i \boldsymbol{\eta}_j^T]$. It should be noted that $\text{Tr}(\Sigma)$ in Proposition 1 provides \mathcal{H}_2 norm of the system in Fig. 2.

Remark 1. It is interesting to observe the system in Fig. 2 from a viewpoint of dynamical multi-agent systems. In Fig. 2, the blocks in the reaction part (upper blocks) are homogeneous block diagonal matrices, and each block diagonal entry $H(s) := (sI - K)^{-1}$ corresponds to the linearized dynamics of intravoxel reactions. It is clear that \mathcal{B}_0 is the noise that perturbs the states of each subsystem $H(s)$. The blocks in the diffusion part (lower blocks), on the other hand, describes the structure of information exchange between $H(s)$. Since S_1 is the incidence matrix associated with the graph Laplacian L , \mathcal{B}_1 can be considered as a perturbation to the sensed output $\boldsymbol{\eta}_{i-1} - \boldsymbol{\eta}_i$. Thus, one might expect that the study of this class of system is useful for engineering applications as well. \square

4.2 Spatial power spectrum analysis of the intrinsic noise

Although the matrix Σ in (15) contains all information about the spatial covariance of $\boldsymbol{\eta}$, it is not easy to see the existence and profiles of spatial pattern at a glance. Hence, we here consider spatial spectrum analysis based on Proposition 1.

The following theorem presents an efficient computation method of the spatial power spectrum of the noise.

Theorem 1. *Consider the system (13). Suppose the spatially homogeneous equilibrium \mathbf{x}^* is locally stable. Let $\boldsymbol{\xi}_i$ ($i = 1, 2, \dots, N$) denote the spatial frequency components of the steady state noise $\boldsymbol{\eta}_i$, i.e.*

$$\boldsymbol{\eta}_i = \sqrt{\frac{1}{N}} \boldsymbol{\xi}_1 + \sqrt{\frac{2}{N}} \sum_{k=2}^N \cos\left(\frac{(k-1)\pi}{N} \left(i - \frac{1}{2}\right)\right) \boldsymbol{\xi}_k. \quad (16)$$

Then, the power spectral density $\Xi_k := \mathbb{E}[\boldsymbol{\xi}_k \boldsymbol{\xi}_k^T] \in \mathbb{R}^{n \times n}$ at the frequency $\omega_k := (k-1)\pi/N$ ($k = 1, 2, \dots, N$) is given by the positive definite solution of

$$\begin{aligned} (K + \lambda_k D) \Xi_k + \Xi_k (K^T + \lambda_k D) + S_0 W_0 S_0^T \\ - 2\lambda_k D W_1 = 0, \end{aligned} \quad (17)$$

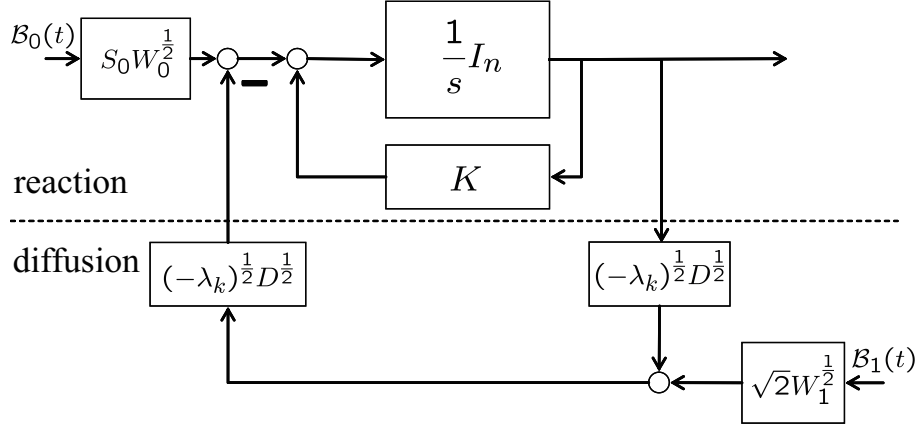


Figure 3: The decomposed subsystem obtained from the large system in Fig. 2.

where

$$\lambda_k := -4 \sin^2 \left(\frac{(k-1)\pi}{2N} \right). \quad (18)$$

We see from Theorem 1 that the spatial power spectral density of the molecule \mathcal{M}_i is obtained as the (i, i) -th entry of the matrices Ξ_k ($k = 1, 2, \dots, N$). In fact, Ξ is obtained by applying discrete cosine transform to the covariance matrix Σ . It should be noted that Ξ_k ($k = 1, 2, \dots, N$) are obtained by solving N Lyapunov equations of the size n by n , which is more computationally efficient than solving nN by nN Lyapunov equation (15) and applying discrete cosine transform.

From a control theoretic viewpoint, the transformation presented in Theorem 1 corresponds to the decomposition of the system into N subsystems as shown in Fig. 3, where $\lambda = \lambda_1, \lambda_2, \dots, \lambda_N$. We see that the feedback gain λ corresponds to frequency ω_k ($k = 1, 2, \dots, N$), and the spatial spectral density Ξ_k varies in terms of λ . Thus, the computation of the spatial power spectrum is essentially the same as \mathcal{H}_2 norm computation for various feedback gains λ .

Since the noise \mathcal{B}_0 and \mathcal{B}_1 are decoupled in Fig. 3, the \mathcal{H}_2 norm can be independently computed for each input. Thus, we have the following proposition.

Proposition 2. *The Lyapunov solution Ξ_k in (17) can be decomposed into $\Xi_k = \Xi_{k1} + \Xi_{k2}$ ($k = 1, 2, \dots, N$), where Ξ_{k1} and Ξ_{k2} are the positive definite solutions of*

$$(K + \lambda_k D)\Xi_{k1} + \Xi_{k1}(K^T + \lambda_k D) + S_0 W_0 S_0^T = 0, \quad (19)$$

$$(K + \lambda_k D)\Xi_{k2} + \Xi_{k2}(K^T + \lambda_k D) - 2\lambda_k D W_1 = 0. \quad (20)$$

It should be noted that Ξ_{k1} and Ξ_{k2} represent the spectral density of the noise originating from intravoxel reactions and diffusion, respectively. Thus, Proposition 2 implies that we can independently analyze the contribution of these noises.

Remark 2. Theorem 1 and Proposition 2 can be applied for systems with the periodic boundary condition. In that case, the Laplacian eigenvalues should be alternatively defined as $\lambda_k = -4 \sin^2((k-1)\pi/N)$, and the solution Ξ corresponds to the discrete Fourier transform of Σ . \square

Table 2: Reactions of the Gray-Scott model

	Reaction	Propensity $w_i(\cdot)$
\mathcal{R}_1	$U_i + 2V_i \rightarrow 3V_i$	$k_1[U_i][V_i]([V_i] - 1)/2\Omega^2$
\mathcal{R}_2	$V_i \rightarrow P_i$	$k_2[V_i]$
\mathcal{R}_3	$\phi \rightarrow U_i$	$k_a u_0 \Omega$
\mathcal{R}_4	$U_i \rightarrow \phi$	$k_a[U_i]$
\mathcal{R}_5	$V_i \rightarrow \phi$	$k_a[V_i]$
	$U_i \rightarrow U_j$ (if $j \in \mathcal{I}_i$)	d_1/ℓ^2
	$V_i \rightarrow V_j$ (if $j \in \mathcal{I}_i$)	d_2/ℓ^2

5 Numerical Simulations

In this section, we first illustrate stochastic Turing patterns induced by intrinsic noise with the well-known Gray-Scott model [13, 14]. Then, we show that the spatial power spectrum analysis presented in the previous section can capture the noisy spatial patterns. Furthermore, we present underlying mechanism of noise-induced Turing patterns based on the system theoretic interpretation given in the previous sections. Due to the limitation of the space, some details are left for our future publication.

5.1 Noise-induced Turing patterns with the Gray-Scott model

The Gray-Scott model consists of the five chemical reactions in Table 2. In reaction \mathcal{R}_1 , U is converted into V , where V catalyzes the production of itself. Then, the reaction \mathcal{R}_2 changes V into the final product form P . The reactions $\mathcal{R}_3, \mathcal{R}_4$ and \mathcal{R}_5 describe the inflow of U from outside, degradation of U and degradation of V .

The deterministic reaction-diffusion model of the Gray-Scott model is given by

$$\begin{aligned} \frac{\partial u}{\partial t} &= -uv^2 + a(1 - u) + d\nabla^2 u \\ \frac{\partial v}{\partial t} &= uv^2 - (a + k)v + \nabla^2 v, \end{aligned} \quad (21)$$

where $u \in \mathbb{R}_+$ and $v \in \mathbb{R}_+$ are normalized concentrations of U and V . The dimensionless constants a, k and d are normalized reaction rates and a diffusion rate defined with the reaction constants in Table 2 as

$$a := \frac{k_a}{k_1 u_0^2}, b := \frac{k_2}{k_1 u_0^2}, d := \frac{d_1}{d_2}. \quad (22)$$

Let the parameters be set as $(u_0, k_1, k_2, k_a, d_1, d_2) = (3.0, 4.0 \times 10^{-2}, 1.98 \times 10^{-2}, 2.16 \times 10^{-2}, 2.16 \times 10^{-13}, 3.6 \times 10^{-14})$, which corresponds to $(a, b, d) = (6.0 \times 10^{-2}, 5.5 \times 10^{-2}, 6.0)$. With this parameter set, both deterministic and stochastic simulations exhibit the spatial pattern as shown in Fig. 4. For the stochastic simulation, the Gillespie's algorithm [18] was used, where the domain was partitioned into $N = 32$ voxels, and the characteristic length and the volume were $\ell = 1.0 \times 10^{-1}$ and $\Omega = 1.0 \times 10^2$, respectively.

We now change the parameter k_2 in the above example to 1.76×10^{-2} , which results in $(a, b, d) = (6.0 \times 10^{-2}, 4.9 \times 10^{-2}, 6.0)$. According to the deterministic analysis [19], a spatially homogeneous equilibrium is stable, hence no spatial pattern is expected. In fact, the deterministic model converges to a homogeneous equilibrium (Fig. 5 (Left)). However,

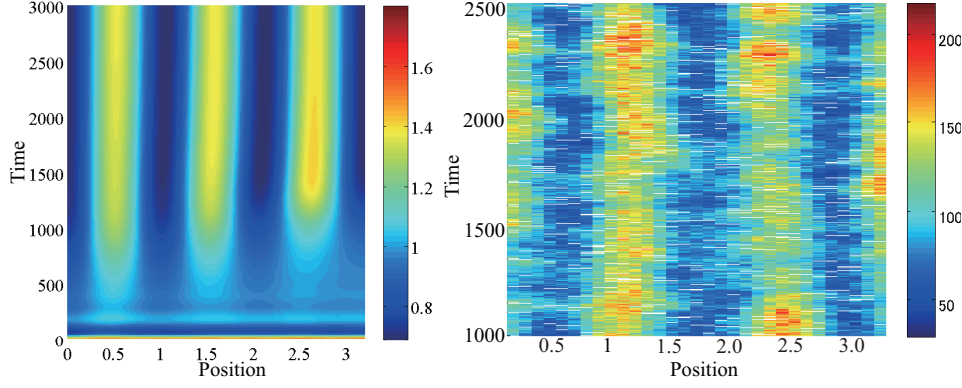


Figure 4: Time development of the concentrations/copy numbers of U for the first parameter set. (Left) A simulation result of the deterministic model. (Right) A result of the stochastic simulation.

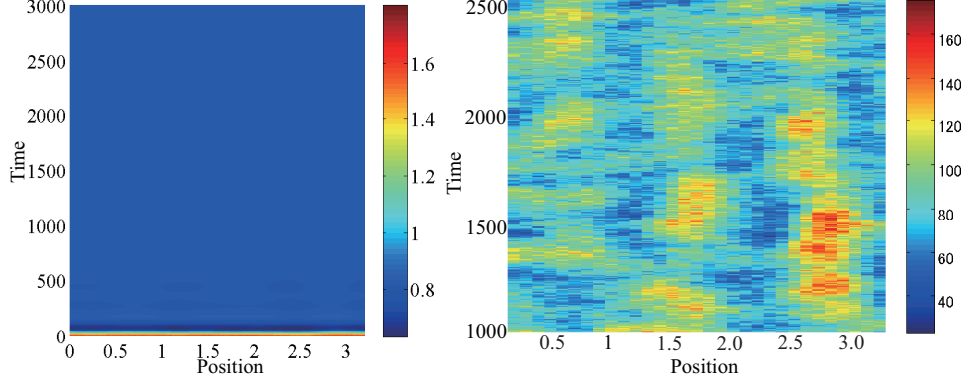


Figure 5: Time development of the concentrations/copy numbers of U for the second parameter set. (Left) A simulation result of the deterministic model. (Right) A result of the stochastic simulation. The red and blue patches imply the existence of noise-induced spatial pattern.

we observe that the stochastic simulation in Fig. 5 (Right) still displays the spatial pattern. It should be emphasized that the deterministic model (21) failed to capture this spatial pattern.

5.2 Spatial power spectrum analysis

In this section, we first show that Theorem 1 and Proposition 2 can capture the stochastic spatial patterns shown in Fig. 5 (Right), then illustrate the mechanism of the stochastic pattern generation from a system theoretic point of view.

Consider the case where the deterministic system (21) does not present Turing pattern. Using Theorem 1, we can approximately compute the steady state spatial power spectrum. Figure 6 shows the computation result in terms of b . We see that as b becomes larger, sharp peak appears at $k = 6$ and 7 , which correspond to $\omega_6 = 5\pi/32$ and $\omega_7 = 6\pi/32$. For $b = 4.9 \times 10^{-2}$, which is the second parameter set in the previous example, the peak frequency

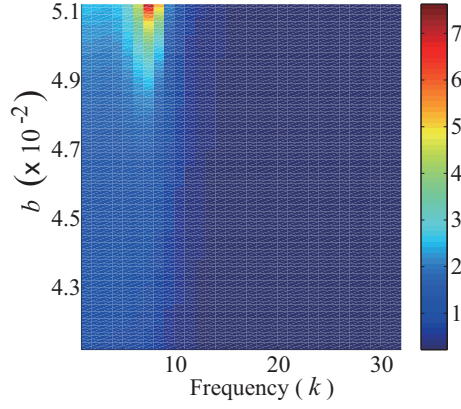


Figure 6: Spatial power spectrum of intrinsic noise $\boldsymbol{\eta}$ computed from Theorem 1. The horizontal axis is k in $\omega_k = (k-1)\pi/N$.

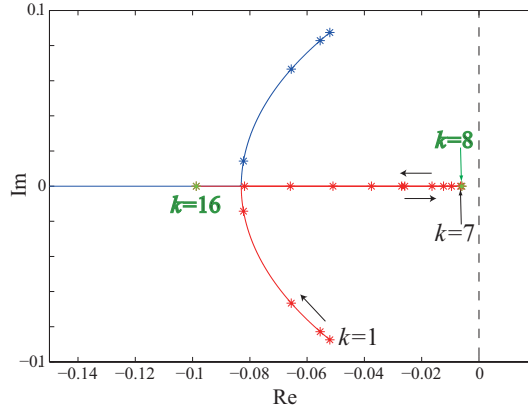


Figure 7: Trajectory of the eigenvalues of $K + \lambda D$ in terms of λ . The mark $*$ stands for the eigenvalues at $\lambda = \lambda_k$.

is ω_7 . Hence, we can expect spatial patterns with three periods. Indeed, the spatial structure can be confirmed in Fig. 5 (Right). The ingredient of the power spectrum can be analyzed with Proposition 2, and it can be concluded that both reactions and diffusion contribute to form the peak at non-zero frequency in Fig. 6

It is interesting to consider these observations from a control theoretic viewpoint. In general, the deterministic Turing instability is determined from the stability of $K + \lambda D$, which corresponds to the stability of the system in Fig. 3. Figure 7 illustrates the eigenvalue distribution of $K + \lambda D$ in terms of λ . Note that this corresponds to drawing the poles of the system in Fig. 3 by changing the feedback gain λ . We see that one eigenvalue approaches to the imaginary axis as k increases, and the largest real part is achieved at $k = 8$ (see Fig. 7). In view of the stability of this system, it is natural that the largest \mathcal{H}_2 norm is obtained around $k = 8$. This observation corroborates the aforementioned analysis illustrated in Fig. 6, where we actually have the peak at $k = 7$.

6 Conclusion

We have analyzed noise-induced pattern formation under the reaction-diffusion kinetics described by the RDME. Using the linear noise approximation, we have revealed the characteristic structure of the stochastic reaction-diffusion system, and presented the underlying mathematical structure of noise-induced pattern formation from a control theoretic point of view. The analytic tool to examine the spatial power spectrum of intrinsic noise has also been derived in the analysis, and its effectiveness has been confirmed through the numerical simulations.

Acknowledgments: This work was supported in part by the Ministry of Education, Culture, Sports, Science and Technology in Japan through Grant-in-Aid for Scientific Research (A) No. 21246067 and Grant-in-Aid for JSPS Fellows No. 23-9203.

References

- [1] A. M. Turing, “The chemical basis of morphogenesis,” *Philosophical Transactions of the Royal Society of London B*, vol. 237, no. 641, pp. 37–72, 1952.
- [2] S. Kondo and T. Miura, “Reaction-diffusion model as a framework for understanding biological pattern formation,” *Science*, vol. 329, pp. 1616–1620, 2010.
- [3] M. B. Elowitz, A. J. Levine, E. D. Siggia, and P. A. Swain, “Stochastic gene expression in a single cell,” *Nature*, vol. 297, no. 5584, pp. 1183–1186, 2002.
- [4] D. T. Gillespie, “A rigorous derivation of the chemical master equation,” *Physica A*, vol. 188, no. 1–3, pp. 404–425, 1992.
- [5] D. Z. Rudner and R. Losick, “Protein subcellular localization in bacteria,” *Cold Spring Harbor Perspectives in Biology*, vol. 2, no. a000307, 2010.
- [6] C. W. Gardiner, K. J. McNeil, D. F. Walls, and F. S. Matheson, “Correlations in stochastic theories of chemical reactions,” *Journal of Statistical Physics*, vol. 14, no. 4, pp. 307–331, 1976.
- [7] T. Biancalani, D. Fanelli, and F. D. Patti, “Stochastic Turing patterns in the Brusselator model,” *Physical Review E*, vol. 81, no. 046215, 2010.
- [8] P. Glandsdorff and I. Prigogine, *Thermodynamic theory of structure, stability and fluctuations*. Wiley, New York, 1971.
- [9] T. Butler and N. Goldenfeld, “Fluctuation-driven Turing patterns,” *Physical Review E*, vol. 84, no. 011112, 2011.
- [10] T. Biancalani, T. Galla, and A. J. McKane, “Stochastic waves in a Brusselator model with nonlocal interaction,” *Physical Review E*, vol. 84, no. 026201, 2011.
- [11] N. G. van Kampen, *Stochastic processes in physics and chemistry*, 3rd ed. North Holland, 2007.
- [12] M. Scott, F. J. Poulin, and H. Tang, “Approximating intrinsic noise in continuous multispecies models,” *Proceedings of the Royal Society A*, vol. 467, no. 2127, pp. 718–737, 2011.

- [13] P. Gray and S. K. Scott, “Autocatalytic reactions in the isothermal continuous stirred tank reactor,” *Chemical Engineering Science*, vol. 39, no. 6, pp. 1087–1097, 1984.
- [14] J. E. Pearson, “Complex patterns in a simple system,” *Science*, vol. 261, no. 5118, pp. 189–192, 1993.
- [15] P. A. Iglesias and B. P. Ingalls, *Control theory and systems biology*. The MIT Press, 2009.
- [16] T. Kurtz, “Limit theorems for sequences of jump markov processes approximating ordinary differential processes,” *Journal of Applied Probability*, vol. 8, pp. 344–356, 1971.
- [17] L. Arnold and M. Theodosopulu, “Deterministic limit of the stochastic model of chemical reactions with diffusion,” *Advances in Applied Probability*, vol. 12, pp. 367–379, 1980.
- [18] D. T. Gillespie, “Exact stochastic simulation of coupled chemical reactions,” *Journal of Physical Chemistry*, vol. 81, no. 25, pp. 2340–2361, 1977.
- [19] W. Mazin, K. E. Rasmussen, E. Mosekilde, P. Borckmans, and G. Dewel, “Pattern formation in the bistable Gray-Scott model,” *Mathematics and Computers in Simulation*, vol. 40, pp. 371–396, 1996.